# THE POLAR IONOSPHERIC X-RAY IMAGING EXPERIMENT (PIXIE)

W. L. IMHOF, K. A. SPEAR, J. W. HAMILTON, B. R. HIGGINS, M. J. MURPHY, J. G. PRONKO and R. R. VONDRAK
*Lockheed Palo Alto Research Laboratories, Palo Alto, CA 94304, U.S.A.*

D. L. McKENZIE, C. J. RICE, D. J. GORNEY, D. A. ROUX, R. L. WILLIAMS and J. A. STEIN
*The Aerospace Corporation, Los Angeles, CA 90009–2957, U.S.A.*

J. BJORDAL, J. STADSNES and K. NJOTEN
*The University of Bergen, Bergen, Norway*

and

T. J. ROSENBERG, L. LUTZ and D. DETRICK
*The University of Maryland, College Park, MD 20742, U.S.A.*

(Received 12 February, 1993)

**Abstract.** The Polar Ionospheric X-ray Imaging Experiment (PIXIE) is an X-ray multiple-pinhole camera designed to image simultaneously an entire auroral region from high altitudes. It will be mounted on the despun platform of the POLAR spacecraft and will measure the spatial distribution and temporal variation of auroral X-ray emissions in the 2 to 60 keV energy range on the day side of the Earth as well as the night. PIXIE consists of two pinhole cameras integrated into one assembly, each equipped with an adjustable aperture plate that allows an optimum number of nonoverlapping images to be formed in the detector plane at each phase of the satellite's eccentric orbit. The aperture plates also allow the pinhole size to be adjusted so that the experimenter can trade off spatial resolution against instrument sensitivity. In the principal mode of operation, one aperture plate will be positioned for high spatial resolution and the other for high sensitivity. The detectors consist of four stacked multiwire position-sensitive proportional counters, two in each of two separate gas chambers. The front chamber operates in the 2–12 keV energy range and the rear chamber in the 10–60 keV range. All of the energy and position information for each telemetered X-ray event is available on the ground. This enables the experimenter to adjust the exposure time *post facto* so that energy spectra of each X-ray emitting region can be independently accumulated. From these data PIXIE will provide, for the first time, global images of precipitated energetic electron spectra, energy inputs, ionospheric electron densities, and upper atmospheric conductivities.

## 1. Introduction

Energetic electrons play a key role in the transfer of energy within the Earth's magnetosphere. They are a major source of ionization of the upper atmosphere and therefore a controlling factor in ionospheric conductivity, which in turn has important implications for the global magnetospheric electrical circuit. Although a variety of possible mechanisms for accelerating these particles have been hypothesized, global measurements with good energy resolution to determine where and when the mechanisms operate have not yet been made.

The Polar Ionospheric X-ray Imaging Experiment (PIXIE) investigation will provide, for the first time, global images of precipitated energetic electron spectra,

*Space Science Reviews* **71:** 385–408, 1995.

energy inputs, ionospheric electron densities, and upper atmospheric conductivities. The PIXIE camera/spectrometer is to be launched on the POLAR satellite and will view an entire hemisphere of the Earth, as one would view a television screen, by remote sensing of the bremsstrahlung X-rays produced by the bombardment of the atmosphere by energetic electrons.

## 2. Scientific Objectives

The Polar Ionospheric X-ray Imaging Experiment (PIXIE) is an X-ray multiple-pinhole camera that makes several nonoverlapping images of the auroral region, which are summed together in ground processing. It will provide global measurements of the spatial distribution and temporal variation of bremsstrahlung X-ray emissions from the Earth's atmosphere. While particle spectrometers can measure electron fluxes directly, they can do so only in the immediate vicinity of a spacecraft. Remote observations detect secondary photons associated with the electron flux; for example, the bremsstrahlung X-rays that are produced when the electrons enter the upper atmosphere. From the PIXIE X-ray measurements, the morphology and spectra of energetic electron precipitation and the effects on the atmosphere can be derived. The measurements can be used to estimate the total rate of electron energy deposition and the energy distribution of the precipitating electrons. The electron energy distribution can then be used to compute the altitude profile of ionization and electrical conductivity. All of these quantities will be derived for the entire northern auroral zone, including any part that is sunlit, simultaneously. PIXIE X-ray measurements, as illustrated in Figure 1, can be made on the day side of the Earth as well as the night, and the precipitating electron intensities and energy spectra can be derived from the X-ray images. These are unique capabilities that cannot be duplicated by visible-range or UV devices. Images of atmospheric bremsstrahlung emission will be obtained over the energy range of 2 to 60 keV. The spatial resolution, which is dependent upon the pinhole size that is selected, will range from 500 to 1100 km when the satellite is at apogee and from 50 to 180 km when the satellite is at perigee. The temporal resolution, which can vary over the auroral scene depending upon the brightness of the individual emitting regions, will range from 1 to 30 min when the satellite is near apogee, with a typical value for a full image being 5 min.

Some examples of phenomena that can be studied with measurements of the emitted X-rays are global energy inputs to the atmosphere from precipitating electrons, spatial/temporal variations in electron precipitation from the outer radiation belt, isolated patches of electron precipitation, spatial/temporal variations in electron precipitation associated with substorms, and global inputs of electron precipitation associated with sudden commencements. These investigations with PIXIE will be enhanced by coordinated studies with other POLAR instruments.

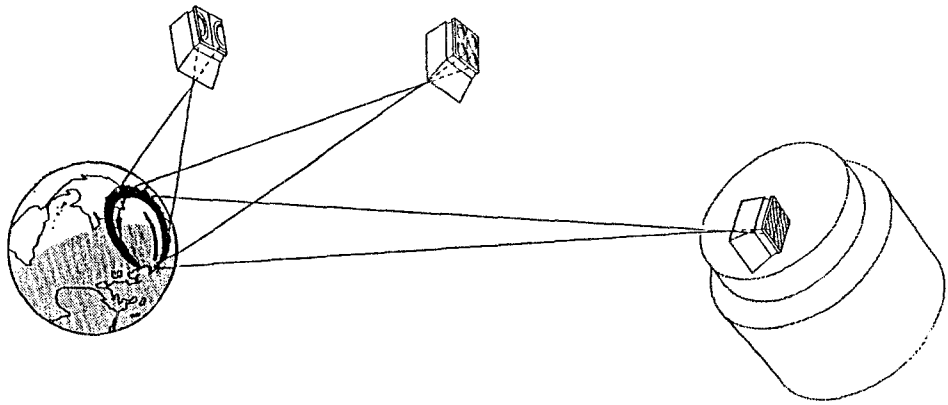

Fig. 1. A schematic drawing of the PIXIE instrument for POLAR that illustrates its unique global mapping capabilities. The selectable pinhole configurations and viewing geometries are shown for three different satellite altitudes. The spatial resolution and the counting rates will be optimized by command at each satellite altitude with the proper selection of the pinhole size and configuration.

The design of the PIXIE instrument and the plans for on-orbit operations and data analysis are based on previous measurements of bremsstrahlung X-rays from satellite altitudes (Imhof *et al.*, 1974, 1985; Imhof, 1981; Datlowe *et al.*, 1988; Mizera *et al.*, 1978, 1984; Gomey, 1987). Previous instruments viewed a relatively small region below a low-altitude spacecraft and, therefore, did not give a global picture, but the data can be taken as representative of certain classes of auroral events. The two physical parameters that are important in describing high-latitude global upper-atmospheric processes are the total energy input to the high latitude regions of the atmosphere and the spectrum of the precipitating electron fluxes that provide a highly variable and significant portion of that energy. Based on the data from low-altitude polar-orbiting satellites, we conclude that bremsstrahlung X-rays can be used to deduce these parameters.

Electrons impinging on the atmosphere lose their energy primarily by collisional ionization of atmospheric species. The small amount of energy loss due to bremsstrahlung is simply related to the ionization loss. Furthermore, the atmospheric density gradient results in a simple relationship between an incident electron's energy and the altitude at which it interacts with the atmosphere. Because of these simple relationships, atmospheric ionization profiles, and therefore electron density and conductivity profiles, can be obtained from bremsstrahlung X-ray spectra. A mapping instrument such as PIXIE can provide separate profiles for each point that is imaged. Figure 2 illustrates some of the results that can be obtained by combining the spatial and spectral information in the PIXIE images. Adding magnetic field measurements by an extensive network of ground-based stations to the conductivities and electron densities derived from the X-ray measurements allows one to determine a variety of parameters describing the polar ionosphere: Hall

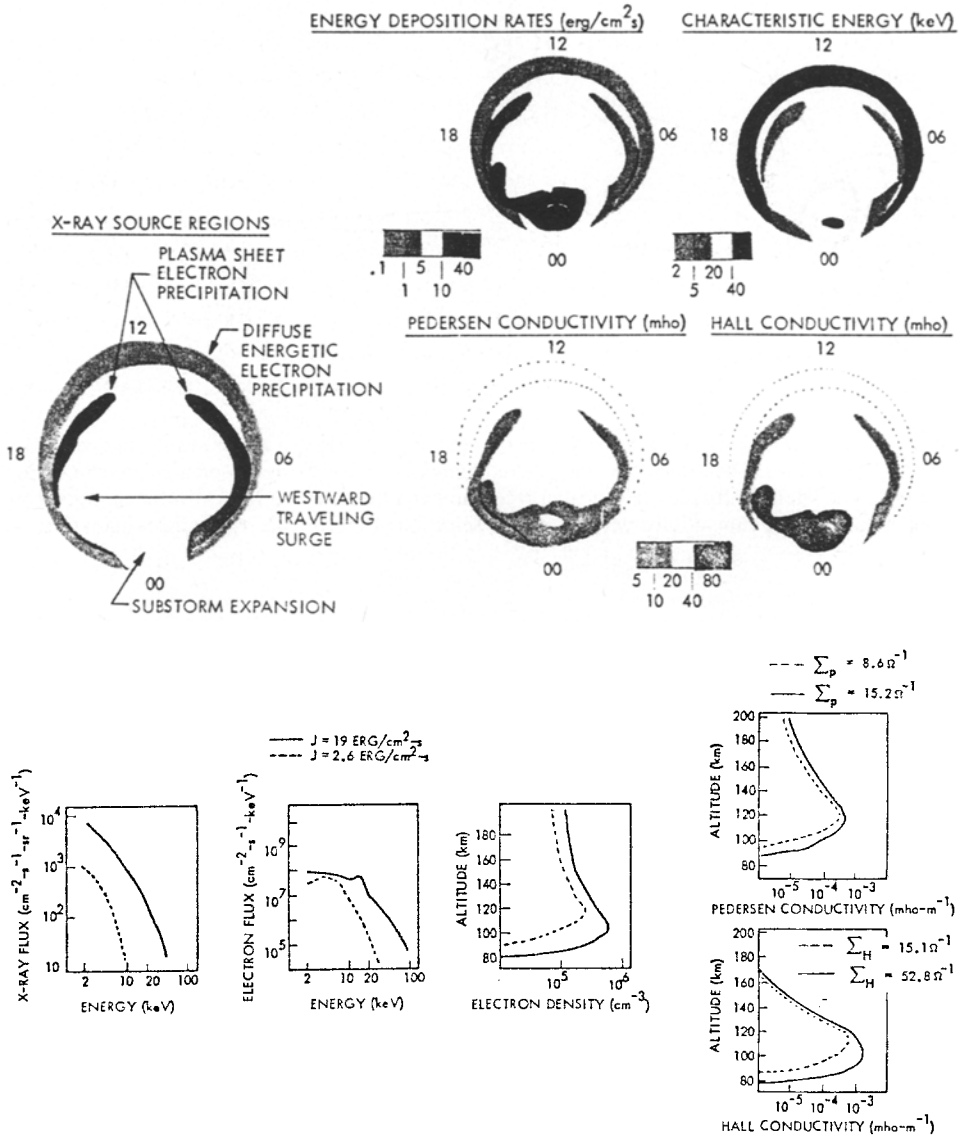


Fig. 2. Expected results from the PIXIE investigation.

and Pedersen currents, field-aligned currents, electric potentials, and Joule heating rates (Ahn *et al.*, 1989). The use of X-ray images permits these parameters to be determined on both the night and day sides of the ionosphere. Imaging at all local times is one of the most important contributions that PIXIE makes to the overall capability of the POLAR scientific payload.

The PIXIE raw data consist of 24 bits of position and energy information for every X-ray event that is detected and telemetered to the ground. In order for an

image to be constructed, each event must be retraced through its corresponding pinhole to an origin point above the surface of the Earth. In this way, individual images are constructed for each open pinhole. The pinhole patterns have been selected to assure that each image point in the detector can be unambiguously associated with one pinhole. The final image is then constructed by adding those associated with all open pinholes. The technique of telemetering all of the information for each event as opposed to onboard image processing has the advantage that it allows the exposure time to be set after the fact, during data analysis. Thus, several images of bright, dynamic, structures can be made simultaneously with a single long exposure of quiescent aurora. In this way it will be possible to obtain point-by-point energy spectra for both bright and faint structures.

The X-ray spectra contain the primary information to be obtained from the PIXIE investigation. The energy spectra of the electrons precipitating into the atmosphere will be derived from the measured X-ray spectra, either by a table look-up technique or by fitting the measured fluxes to an assumed functional form. Whichever method is chosen for routine processing of the PIXIE data, other methods will be developed that will allow for a more accurate determination of the energy spectrum when the count rates are sufficiently high.

## 3. Instrument Description

### 3.1. Conceptual Design

The PIXIE instrument, illustrated in Figure 3, is a multiple-pinhole X-ray camera using a multiwire position-sensing gas proportional counter for the focal plane detector. The instrument is designed to cover an energy range from 2 to 60 keV with a $\pm 21$ deg field of view. The instrument uses multiple pinholes to project nonoverlapping auroral images onto the focal plane. The number and size of the pinholes are selectable via movable aperture plates, enabling the field of view and sensitivity to change as the POLAR satellite moves from perigee to apogee in its highly eccentric orbit. PIXIE will be located on the POLAR satellite's despun platform.

PIXIE is a step in the evolutionary development of instruments designed to image the aurora in hard X-rays; here, 'hard X-rays' means those of high enough energy to make the use of grazing-incidence optics impractical or impossible. Previous instruments flown aboard satellites in low-Earth orbit have built up one image per orbit of part of the auroral zone either by scanning a single detector cross-track (DMSP F-6 GFE-6 instrument: Mizera *et al.*, 1984) or by using a pinhole and a one-dimensional (cross-track) array of detectors (UARS PEM/AXIS instrument: Chenette *et al.*, 1992) or a one-dimensional position-sensitive proportional counter (SEEP/XRIS instrument: Calvert *et al.*, 1983). Two-dimensional hard X-ray imagers have been flown on high-altitude balloons (Mauk *et al.*, 1981;

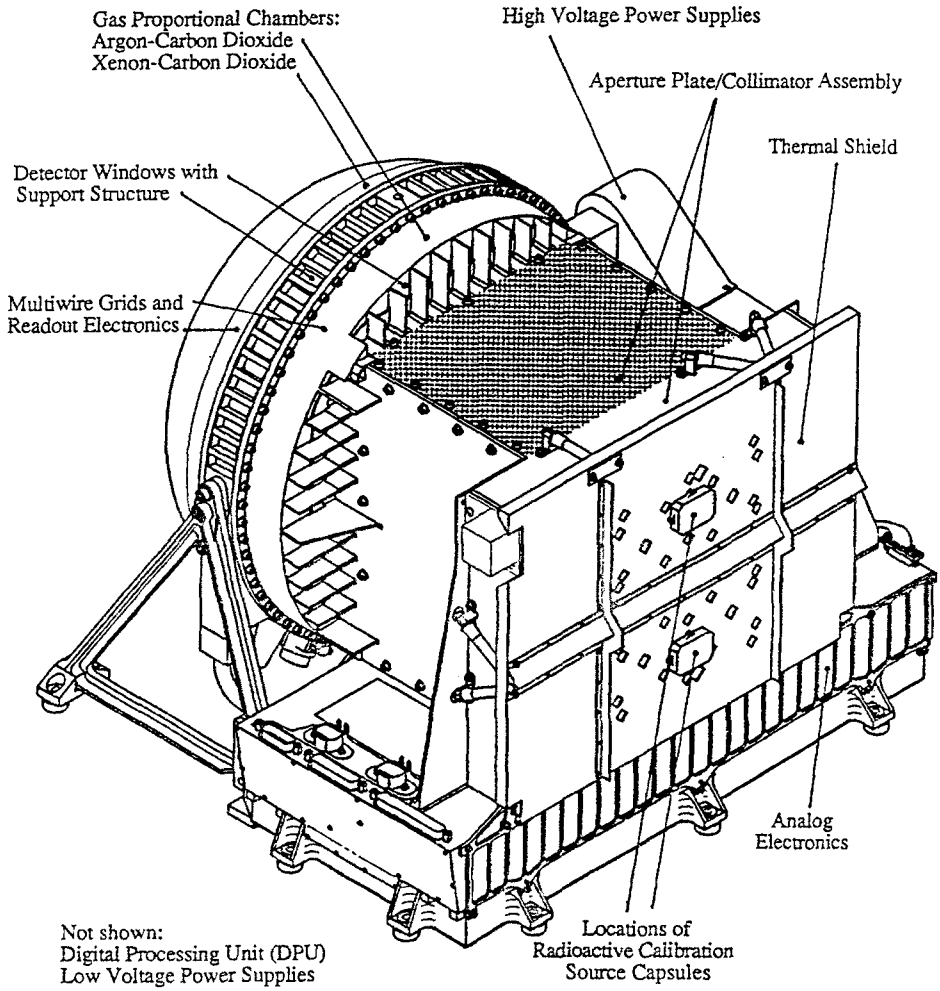


Fig. 3. The PIXIE camera.

Yamagami *et al.*, 1990). PIXIE's heritage also includes coded-aperture instruments (Mertz and Young, 1961), which produce overlapping images on a two-dimensional position-sensitive proportional counter (Skinner *et al.*, 1988) or gas-scintillation proportional counter. Coded-aperture systems are most effective when the source is compact and has high contrast. When the source region is large and diffuse, like the auroral ovals, the combined sensitivity and image contrast for a multiple-pinhole system becomes comparable to that of a coded aperture. The advantages of a multiple pinhole system over a coded aperture include the ability to adjust the spatial resolution and field of view, the ability to vary exposure time from point to point in the image, and a simple image reconstruction process.

The weight, volume, power, and telemetry allocation are optimized within satellite resources. The PIXIE instrument mass is 24.5 kg, the power allotment is

11.0 W (with an additional 8 W on a duty cycle of approximately 3.5% used to move the aperture plates), and the telemetry rate is 3.5 kbps.

### 3.2. COLLIMATOR AND PINHOLE APERTURE PLATES

The fundamental objective of the PIXIE program is to obtain global (i.e., one entire polar region) images of the aurora in the X-ray region of the spectrum. The POLAR satellite has an eccentric orbit such that the distance between the satellite and the aurora varies between roughly 0.8 and 8 $R_E$ ($R_E$ = Earth radius). The result is that the solid angle subtended by the aurora varies greatly, producing an image of the auroral oval on the detector that is small when the satellite is near apogee and large near perigee. Furthermore, the auroral X-ray fluxes at high altitude are weak, so the PIXIE camera is signal limited. The use of the selectable aperture allows PIXIE to make optimum use of the weak X-ray flux by having the selectable aperture open more pinholes at high altitudes than at low altitudes. Since the auroral solid angle is smaller when the satellite is at higher altitude, more nonoverlapping images can be placed on the detector at higher altitudes (see Figure 1). A second function of the selectable aperture is to vary the size of the pinhole openings, thereby allowing the experimenter to trade off the camera's angular resolution against sensitivity. (A 'zoom' lens accomplishes these same objectives with a variable focal length.) The PIXIE design incorporates a dual aperture system so that one-half of the camera assembly can operate with high sensitivity (large pinholes) while the other simultaneously operates with high spatial resolution (small pinholes). Of course, it is also possible to operate the whole camera in either of these two modes.

Figure 4 is a view of the outer, fixed, PIXIE aperture plate. The pinholes are shaded and labeled with 'H' (high altitude), 'M' (mid altitude), and 'L' (low altitude) according to the phase of the orbit at which they are opened. Thus, near apogee, the 'H' pinholes are opened to produce 16 nonoverlapping images of the auroral scene on the detector. Sets with fewer pinholes are successively opened as the satellite's altitude is reduced. There is, in addition, a pair of pinholes labeled 'P' (for perigee) for use when the satellite is near perigee. Currently, the operational plan calls for the open pinhole set to be changed when the individual images of a circle of diameter 1 $R_E$ at the Earth would just begin to overlap. This policy allows for nonoverlapping images of a very active aurora, and on-orbit experience may cause us to adopt a less conservative criterion for changing the pinhole configuration. In any case, the points at which the aperture plates are repositioned are functions of the orbit phase and will not vary from orbit to orbit. The selectable aperture is mounted atop the PIXIE detector so that the hole pattern faces the auroral scene to be imaged. Each pinhole set is centered over the detector. The position-sensitive sealed proportional counter fulfills the role of film in the pinhole camera. The aperture plates and all of the collimator panels are made of a special X-ray absorbing laminate designed specifically for the PIXIE instrument.

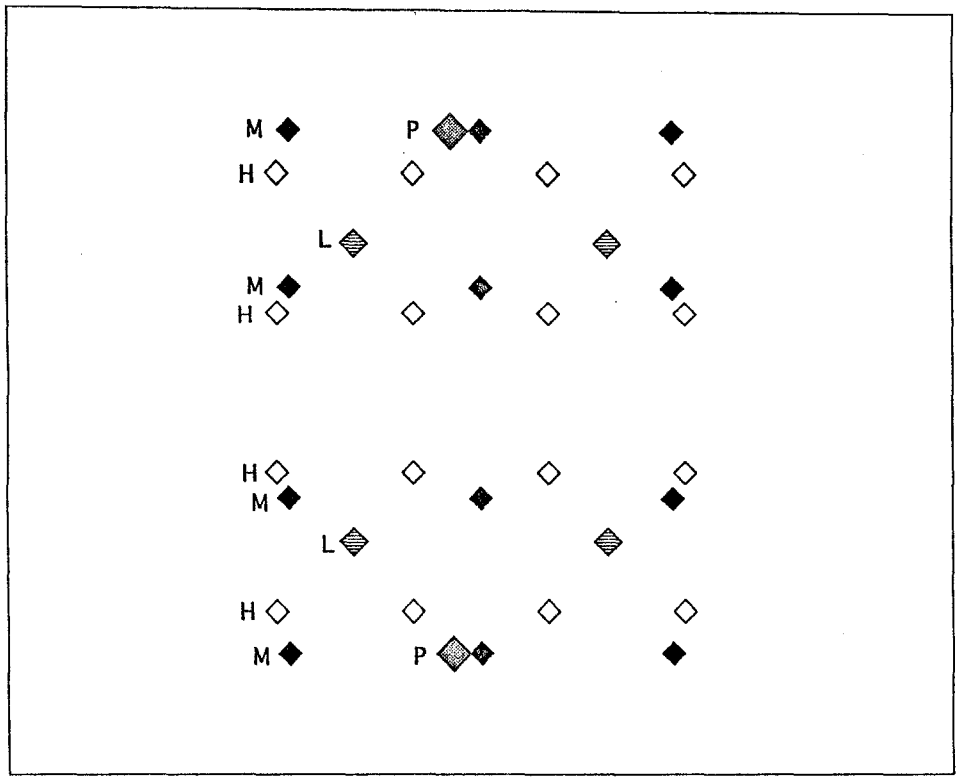


Fig. 4. The fixed aperture plate. The pinholes are labeled and shaded according to their membership in the high (H), mid-altitude (M), low (L), or perigee (P) set.

Figure 5 helps in explaining the operation of the aperture plate. The figure shows both the fixed plate and the two movable plates, with the movable plates outlined in dashes and the movable-plate holes shaded. X-rays pass through the pinholes at those points where two holes overlap. In the figure, the lower plate has been positioned for viewing from low altitude, while the upper remains in the mid-altitude configuration. This transition would be made when the satellite is at a distance of approximately 6.6 $R_E$ from the center of the Earth. The medium-altitude holes are relatively wide open, which would correspond to higher sensitivity, while the low-altitude holes are not as wide open and are the 'high-resolution' set. The two movable plates and all of the plate-motion mechanisms are beneath the fixed plate and are entirely contained within the collimator structure. For the half of the camera associated with each aperture plate, there are eight holes in the high-altitude set and two in the low-altitude set. The mid- altitude set consists of six holes for each camera half, but the three holes in each set that are located along the outer edge of the camera image slightly more than one-half of the auroral scene and are therefore regarded as half-holes. Thus there are effectively $4\frac{1}{2}$ mid-altitude holes in each camera half. Similarly, the large perigee holes, one in each camera half, image

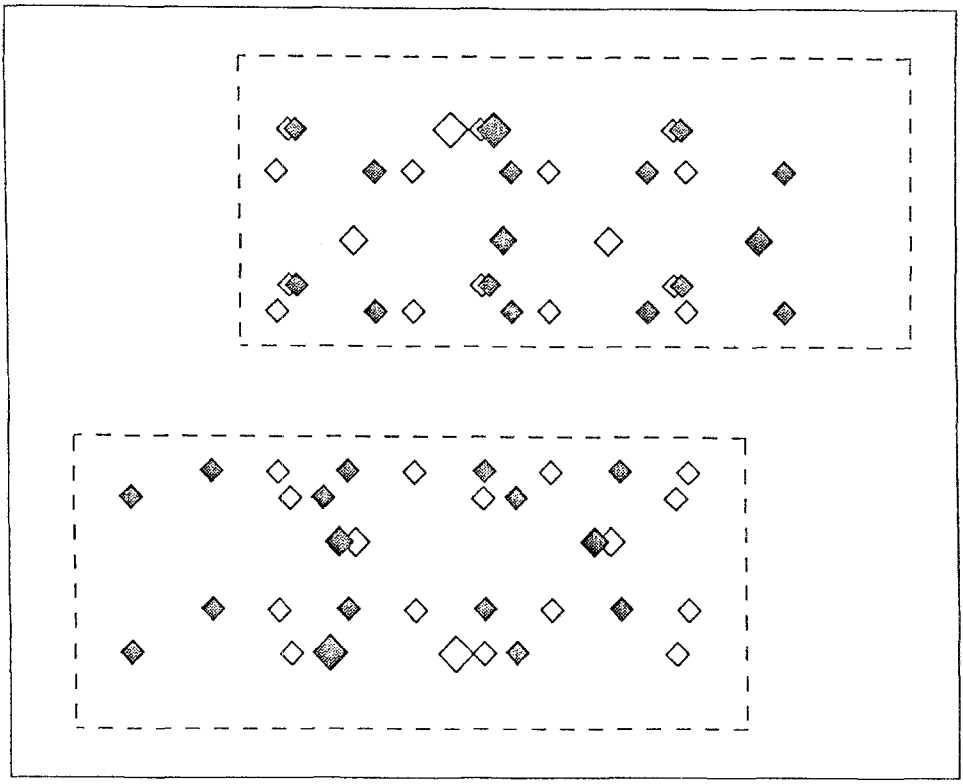

Fig. 5. The fixed and movable aperture plates. The movable plates are outlined with dashes, and have shaded holes. The upper movable plate is positioned for mid-altitude viewing with high sensitivity, and the lower is positioned for low-altitude viewing with high spatial resolution.

slightly more than half the scene, so there is effectively one perigee pinhole for the whole camera. For the multiple-pinhole subsets, a single image is constructed by summing the images from the individual holes. The holes are tapered, as shown in Figure 6, so that the extreme off-axis rays are parallel to the sides of the holes, and the effective area of the hole varies slowly, only as the cosine of the off-axis angle. Not shown in Figure 5 are two radioactive calibration sources for each camera half, which are located on the fixed aperture plate (the source capsules can be seen in Figure 3). The sources are uncovered by positioning a calibration hole (not shown) on each movable plate beneath the sources. All imaging pinholes are closed during calibration.

Each aperture plate is positioned by a lead-screw mechanism that is driven by a stepper motor with a reduction gear-head. The position of the plate is determined by the step count from the opening of a limit switch at the home position at the end of travel. Whenever a plate is repositioned, it is first driven back to 'home' to re-establish this fiducial starting point. The position-selection resolution is 0.02 mm. Since the plate motion is across the diagonal of the hole, the hole-size resolution is

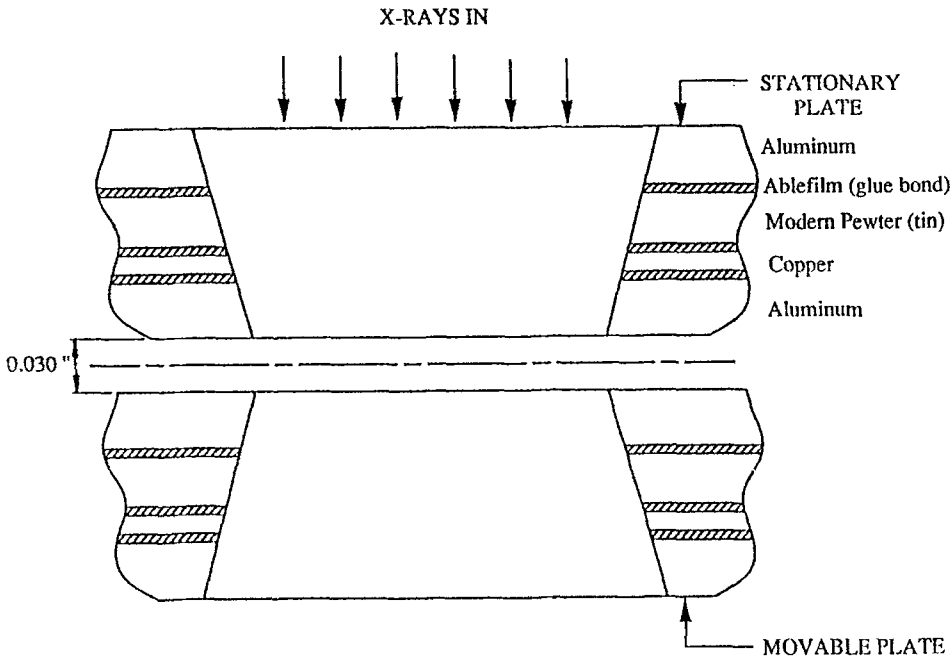


Fig. 6. Cross section of the aperture plate holes.

better by a factor of $\sqrt{2}$. Each plate has a linear potentiometer that can be read out with a resolution of 0.31 mm, which is inadequate for plate positioning but gives an indication in telemetry that the plate motion has actually occurred as commanded. Each aperture plate is equipped with two redundant limit switches at each end of travel. Either end of travel can serve as the fiducial 'home' position, so the system is highly redundant. Even with the unlikely occurrence of a total failure of one driver system, the instrument retains 50–86% of its data-gathering capability, depending upon the position of the failed plate at the time of failure.

### 3.3. Position-Sensitive Proportional Counter

The PIXIE focal plane detector is a multiwire gas proportional counter (MWPC), shown schematically in cross section in Figure 7. It is designed to be sensitive to X-rays in the energy range from 2 to 60 keV. To maximize absolute efficiency over the full energy range, the counter has been subdivided into a one- atmosphere front chamber filled with $Ar/CO_2$ with a 4 mil thick Be entrance window, and a two-atmosphere rear chamber of $Xe/CO_2$ separated from the front argon chamber by an 80 mil thick Be window. This subdivided design has the added reliability advantage of two independently operable chambers.

Within each chamber is an interleaved stack of two anodes and three cathodes that defines two independent active regions (see Figure 7). The anodes are operated at positive high voltage and provide the X-ray energy information; the cathodes

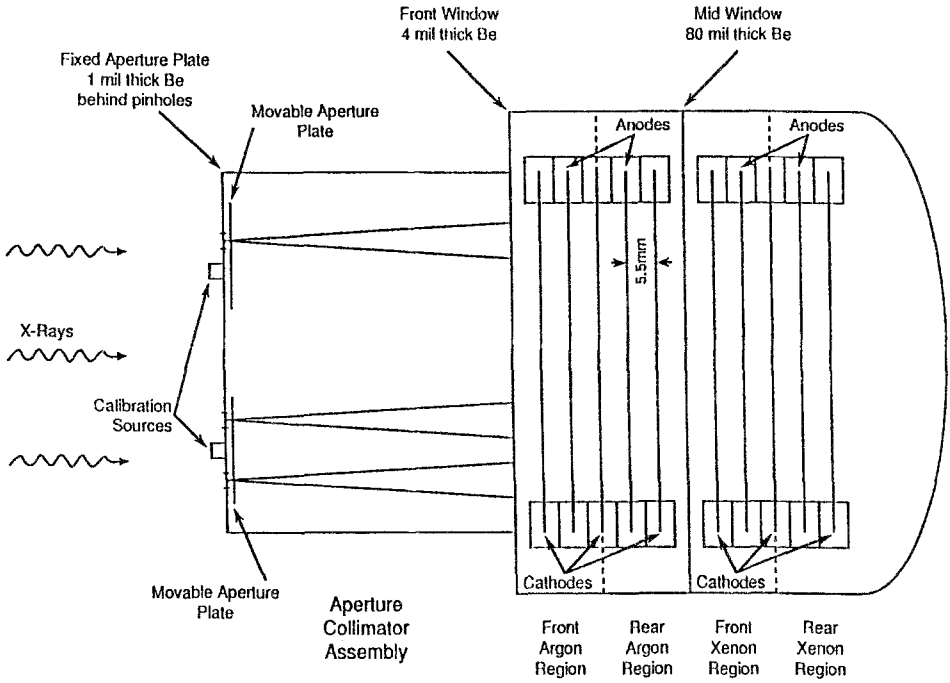


Fig. 7. Cross sectional schematic of the PIXIE multiwire proportional counter.

are held at ground potential and are used to determine the $(x, y)$ position of the interaction of the X-ray photon with the chamber gas as described in more detail in Section 3.4. The anode collects the charge from all events occurring in the volume between its two adjacent cathodes.

The overall active area of the counter is $18 \times 18$ square cm, and the total active depth is 4.4 cm. The spatial resolution is $\approx 2$ mm (FWHM) over nearly the entire detector area. In order to preserve good position resolution for X-rays entering the detector at angles up to 21 deg off normal incidence, the anode/cathode separation has been restricted to 5.5 mm.

Each anode consists of 90 gold-plated tungsten wires of 12.5 micron diameter separated from one another by 2 mm. The two outermost wires on each side are used independently for background discrimination; the rest of the wires on each anode are connected together and to a common amplifier to provide the total energy signal. Each cathode plane has 179 gold-plated tungsten wires separated from each other by 1 mm. The top and bottom cathodes in each chamber have 30-micron wires, while the center cathode has 50-micron wires oriented perpendicular to the wires of the other two cathodes to provide $(x, y)$ position coordinates. The position determination is made using a graded-density wire pattern for the cathodes, which will be discussed in more detail in the following section.

The proportional counter quench gas is $CO_2$ rather than an organic molecule such as methane; this eliminates the problem of radiation-induced cracking of

TABLE I
Detector parameters

| | | | |
|---|---|---|---|
| Active detector area | 180 mm × 180 mm | | |
| Anode – cathode separation | 5.5 mm | | |
| | Anode | Center cathode | Top and bottom cathodes |
| Number of signal wires | 86 | 175 | 175 |
| Signal wire diameter | 12.5 $\mu$m | 50 $\mu$m | 30 $\mu$m |
| Number of edge wires | 2 + 2 | 2 + 2 | 2 + 2 |
| Edge wire diameter | 12.5 $\mu$m | 100 $\mu$m | 100 $\mu$m |
| Wire separation | 2 mm | 1 mm | 1 mm |
| Wire material | Gold plated tungsten with 3% rhenium | | |

organic molecules and their subsequent polymerization in the high fields surrounding the anode wires, which is a well-known cause of counter degradation and failure. Still, all proportional counters are limited in the total amount of ionization they can experience; therefore the PIXIE high voltage bias will be turned off during passage through the radiation belts. Furthermore, electronic circuits will monitor the count rates at all times and shut down the high voltage whenever anomalously high counting rates are experienced.

Weight and volume restrictions preclude the use of a recirculating gas purification system for the proportional counter. Therefore the instrument uses sealed stainless steel chambers and low outgassing materials to minimize the possibility of gas contamination. So long as the chambers have no significant leaks and no catastrophic failures, the above measures assure that degradation of the detectors will not limit the instrument life to less than a three-year POLAR mission.

The overall detector parameters are summarized in Table I.

### 3.4. GRADED DENSITY POSITION READOUT

The position readout system is based upon the use of graded density (GD) cathodes (Mathieson *et al.*, 1980). The simplicity of the design and the minimal number of electrical components required on the wire frames make this method well suited for use in sealed gas chambers where contamination cannot be tolerated. The response function of the GD cathode is mainly dependent on well controlled mechanical design parameters.

The principle of operation of a one-section GD cathode is shown schematically in Figure 8(a). Each cathode wire is electrically connected to one of two possible signal outputs, A or B. The spatial densities of 'A-wires' and 'B-wires' vary linearly from one side of the cathode to the other. An electron avalanche on an anode wire will induce electrical charges on a number of wires on the neighbor cathodes, as schematically indicated by the superimposed bar diagram. The spatial distribution

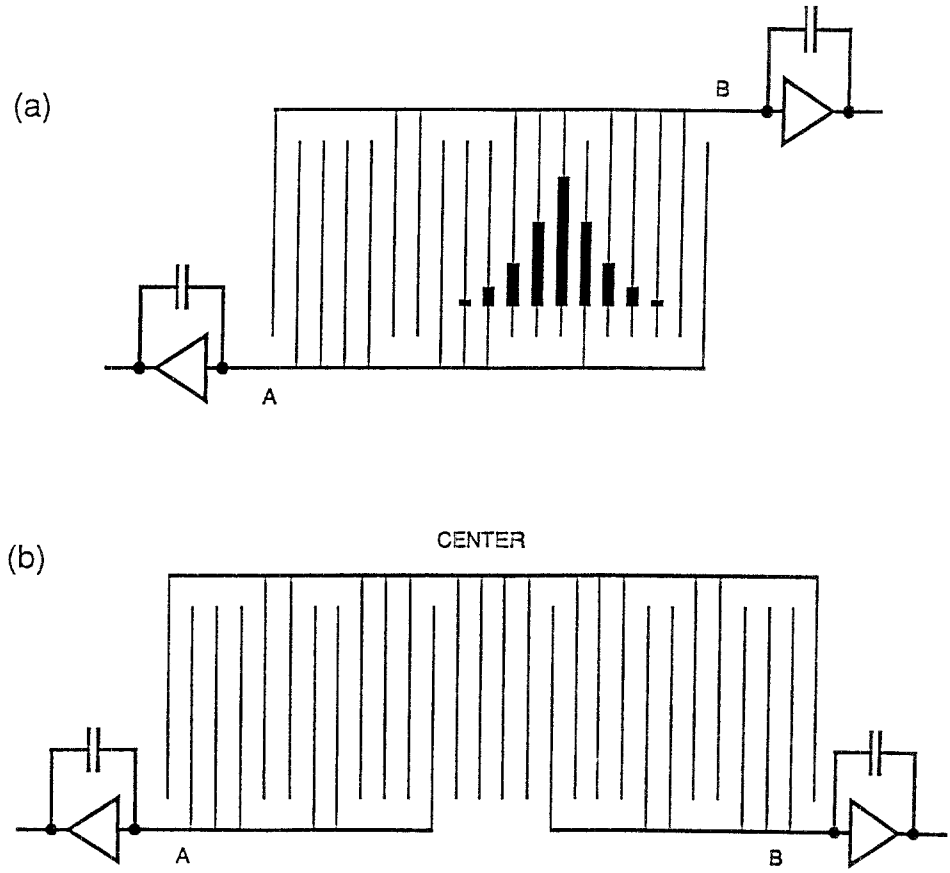


Fig. 8. Schematic representation of the operation of a graded density cathode.

of the charges will have a width of the order of the separation between anode and cathodes. The total charge induced on the A cathode wires is denoted $q_A$, and that induced on the B wires is denoted $q_B$. The individual A and B cathode wires are distributed in such a way as to cause the ratio of the output charge signals, $q_B/(q_A + q_B)$, to vary linearly with the position of the electron avalanche event. The use of two GD cathodes. one in the $x$-dimension and the other in the $y$-dimension allows the site of the initial X-ray interaction to be located within a 2-mm uncertainty. The $z$-dimension is identified with the anode plane on which the interaction was recorded, with an uncertainty of $\pm 5.5$ mm.

The position linearity of a one-section GD cathode deteriorates if the number of cathode wires becomes large. PIXIE therefore uses a refined version of the system with two cascaded GD sections on each cathode plane (Gilvin *et al.*, 1981). This design is shown schematically in Figure 8(b). The charge division between A and B is accomplished by their capacitive coupling through the center section. The design

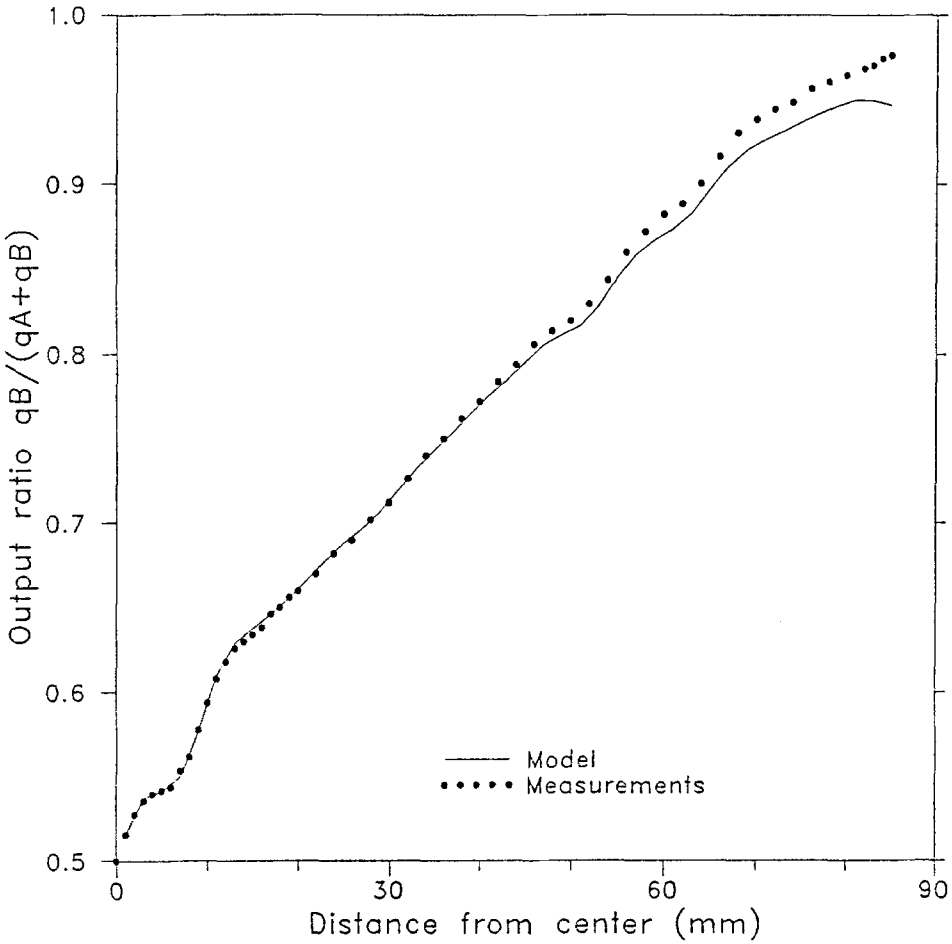


Fig. 9. Output signals versus position of the X-ray beam for a graded density cathode.

has the advantage of reducing the detector capacitance, but in order to maintain a near linear spatial response the wire grading has to be made nonlinear.

An example of the observed position signal versus the position of a tightly collimated X-ray beam for a laboratory prototype of the PIXIE detector is shown in Figure 9. The relationship is symmetrical about the center of the detector. The behavior of the cathode can be closely described by model calculations. The deviations between model and observations at large distances from the center are caused by coupling capacitances that were not included in the model.

### 3.5. Background and Shielding

The POLAR satellite orbit will expose the instrument to the primary cosmic X-ray and charged-particle background, as well as the Earth's radiation belts (which will

induce radioactivity in the detector and its surrounding materials). Potential sources of X-ray background include bremsstrahlung produced by electrons striking the satellite structure, the diffuse component of cosmic X-rays, and solar X-ray albedo from the Earth's atmosphere. The instrument design includes passive shielding for X-rays and active charged- particle background rejection. Passive shielding is adequate to prevent cosmic X-rays from being a significant background source at energies below 45 keV; at higher energies their contribution is comparable to that of unvetoed cosmic-ray interactions. The solar X-ray albedo, some of which occurs within the instrument's field of view, is of such low intensity that it can be ignored as a background source. The instrument will be shut down during each passage through the radiation belts, primarily to protect the detectors from degradation. Despite the shut-down in the radiation belts, PIXIE will provide several hours of continuous observations of the polar atmosphere while it passes through apogee and approximately one-half hour of perigee observations per orbit. The time available for continuous global observations is much longer than the typical duration of a magnetospheric substorm, which is the most prominent manifestation of electron energy deposition into the upper atmosphere.

To reduce X-ray background the collimator box has been designed with layers of materials of different atomic number to absorb secondary fluorescent X-rays, and an internal baffle prevents the detector from viewing the satellite structure directly through the pinholes. Likewise on the rear dome the chamber steel is overlaid with silver to increase absorption without increasing the effects of fluorescence. To reduce the charged-particle background, the instrument includes electronic logic to recognize coincident anode events. Any event that triggers a signal on more than one anode will be recognized as a charged particle and electronically rejected. Furthermore, the outermost two wires on each of the anode and center cathode wire planes will be operated independently as edge wires guarding against cosmic rays entering through the sides. Any event that triggers an edge wire will be electronically rejected. This composite rejection scheme will veto 99% of the cosmic ray background in the rear argon and front xenon active regions, and 85 to 90% in the front argon and rear xenon active regions (see Figure 7). Even so, unrejected cosmic-ray events are expected to be the most important background contributor to PIXIE.

### 3.6. Electronics and Data Handling System

The PIXIE electronics, shown in Figure 10, can be divided into five sections: (1) the Low-Voltage Power Supplies (LVPS) to provide power to the entire instrument; (2) the High-Voltage Power Supplies (HVPS) to bias the detectors; (3) the Signal Processor Unit (SPU) analog section, which amplifies and holds the detector signals, and perforrns the analog division required for determining the position of the X-ray events; (4) the SPU digital section, which selects the valid events, controls event processing, and digitizes the event data; and (5) the Data Processing Unit

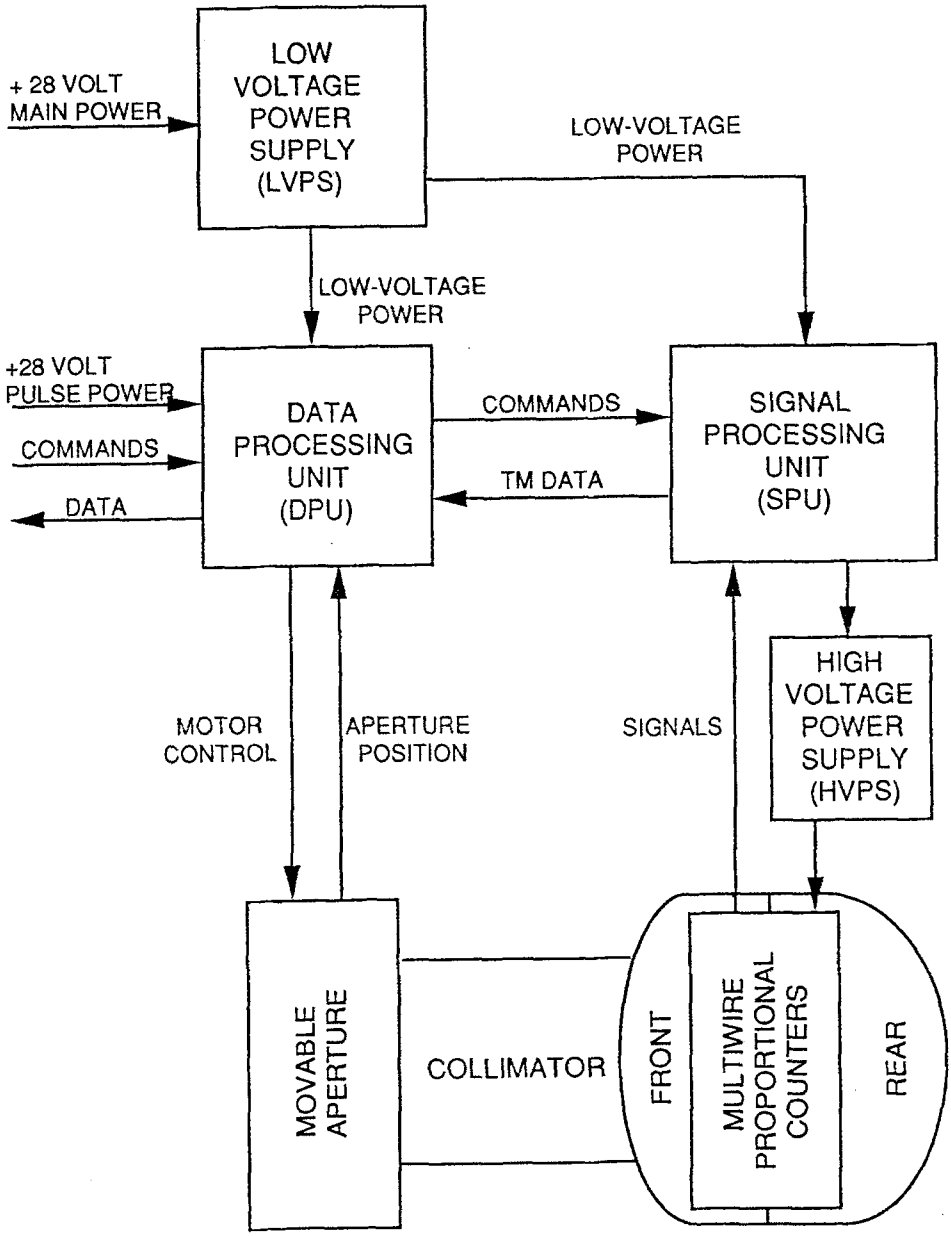


Fig. 10. PIXIE system block diagram.

(DPU), which buffers the data and routes it to telemetry, processes aperture-system commands, and controls the aperture positioning.

There are two high-voltage power supplies, one for each chamber. They are individually enabled by command and programmable to one of 64 voltage steps that cover the top 40% of their voltage ranges. The control circuitry also includes a

high-rate-sensing circuit that tums off the high voltage whenever the counting rate in the detector exceeds a predetermined count rate. Proportional counters have a finite lifetime in terms of integrated counts, and these circuits protect the detectors from situations such as a failure to command the high-voltage off when the satellite enters the Earth's radiation belts or encounters unexpectedly high radiation fluxes outside the belts. A second protection circuit is designed to detect sparking and disable the supplies. These protection circuits are enabled and disabled by ground command. When the high voltage is turned off by one of the protection circuits, the instrument waits for a predetermined period and then turns on the high voltage again.

The analog section of the SPU handles the signals that come from the detector. The proportional counter signals consist of a total of four anode energy signals (two from each chamber, see Section 3.3), six pairs of cathode position signals ($q_A$, $q_B$) (three pairs from each chamber, see Section 3.4), four anode edge wire signals (one from each anode, see Section 3.5), and four cathode edge wire signals (two from the center cathode in each chamber, see Section 3.5). For each cathode, the interaction position is linearly related to the ratio $q_B/(q_A + q_B)$ of the two cathode signals.

The SPU electronics includes 24 amplifier chains with charge-sensitive preamplifiers and shaping amplifiers. Event selection is performed by making use of upper and lower-level discriminators (ULD's and LLD's) in the signal-processing chains. The signal processing is set in motion when one of the anode LLD's is triggered. All events that trigger more than one anode LLD or an edge-wire LLD or that lie outside the anode discriminator window are vetoed as background. Thus an event is processed if it activates one and only one anode, none of the edge-wire LLD's, and none of the anode ULD's. (Telemetry limitations require that valid events be selected electronically in the instrument.) All of the veto functions can be disabled by ground command if necessary. In addition, each edge-wire LLD threshold can be individually adjusted to one of four levels by command.

The digital electronics in the SPU perform the analog-to-digital conversion of the position and energy information and assemble the 24 bits of digital data that characterize each validated X-ray event. As described above, the $x$ and $y$ coordinates of the initial X-ray interaction are determined from the graded-density cathode signals by performing the analog division, $q_B/(q_A + q_B)$. The ratio is digitized by an analog-to-digital converter with 10-bit precision. The ten-bit output from each ADC is routed to a PROM that uses a look-up table to linearize and compress the data to eight bits. The use of the look-up PROM is required because of nonlinearities in the graded-density cathodes (see Figure 9). The resulting position data have precision of 180/256 = 0.70 mm, approximately three times finer than the intrinsic detector spatial resolution of 2 mm. Two additional bits identify which of the four anodes recorded the signal ($z$-coordinate). Six bits of energy information are obtained by an ADC that digitizes the anode pulse height. Thus the front and rear detectors have 64 channels over the energy ranges 2–12 and 10–60 keV,

respectively. The energy resolution of the MWPC is $\approx$ 25% FWHM at 6 keV in the front chamber and $\approx$ 30% FWHM at 12 keV in the rear chamber, so the energy is read out with a precision much finer than the detector resolution.

There are two basic methods of telemetering the image data: (1) processing the data on-board and periodically telemetering processed images in selected energy bins; or (2) telemetering all of the information (24 bits in this case) for each valid X-ray event individually. PIXIE uses event-by-event telemetry. This method is preferable whenever adequate bandwidth is available (as it is for PIXIE) because it provides the experimenter with a great deal of flexibility in data reduction and analysis. The exposure time can be selected after the fact and can even be different for different parts of the image. This permits one to integrate for longer periods of time on faint quiescent structures. The full 64-channel energy resolution is available and energy binning can be done on the ground. Similarly, the image pixels can be binned. Both energy and spatial binning (to provide a common scale for images taken at different phases of the orbit) will be used in constructing the key-parameter images that PIXIE will provide to the International Solar-Terrestrial Physics Program Central Data Handling Facility. All of the PIXIE image construction will be done on the ground, including summing of the images that are associated with the individual pinholes.

When the SPU has finished processing a valid X-ray event, it places the 24 bits of information in a buffer and signals the DPU that data are ready for transfer to telemetry. The data are transferred in three bytes on an eight-bit bus and are stored in a 4-by-24-bit buffer in the DPU. Buffer-control logic in the DPU assures that the new data do not overwrite data that have not yet been telemetered and also sequences the data transfer to telemetry. The buffer depth provides optimum protection against data loss due to telemetry dead time without requiring excessive circuitry. The PIXIE telemetry bandwidth of 3.5 kbits $s^{-1}$ allows 135 events $s^{-1}$ to be telemetered.

In addition to the event data, there are 20 16-bit scalers that count the number of events in the detectors. The four anode LLD event totals are telemetered with 0.92-s resolution, and the following totals are provided with 4.6-s resolution: edge LLD (8), anode ULD (4), total 'good' events, total rejected events, total events rejected because of anode ULD triggering, and total events rejected because multiple anode LLDs were triggered. The DPU also includes an ADC that digitizes a variety of analog voltages (thermistors, voltage monitors, and so forth). These housekeeping data and a number of digital status bytes are included in the telemetry. Finally, the DPU controls the pinhole aperture adjustment as discussed in Section 3.2.

### 3.7. INSTRUMENT SENSITIVITY

In order to evaluate the sensitivity of the PIXIE instrument to realistic magnetospheric conditions, we made use of computed auroral X-ray luminosities (Miller

and Vondrak, 1985). The calculations were performed using a model that specifies the instantaneous pattern of electron precipitation, as well as the temporal variations during a magnetospheric substorm. Seven types of auroral sources were assumed in the phenomenological model. The diffuse aurora and discrete arcs are present under all conditions. The other five forms (bright arcs, bright diffuse aurora, enhanced 'dawn drizzle', westward traveling surges, and postbreakup emission) occur during the active phases of a substorm.

The sensitivity of the PIXIE instrument varies rapidly with the size of the pinholes. In the final image, the instrument geometric factor is $n_p s^4/f^2$ per resolution element, where $n_p$ is the number of pinholes (i.e., the number of single-pinhole images that are summed to make the final image), $s$ is the linear size of the (square) pinhole, and $f$ is the 'focal length' (21 cm). For the high, medium, and low-altitude, and perigee pinhole sets, $n_p$ = 16, 9, 4, and 1, respectively, and the maximum values of $s$ are 0.47, 0.47, 0.57, and 0.70 cm, respectively. Therefore, the maximum geometric factors for the four sets, in the order listed above, are $1.8 \times 10^{-3}$, $1.0 \times 10^{-3}$, $1.0 \times 10^{-3}$, and $5.4 \times 10^{-4}$ cm$^2$ sr. For practical purposes, the maximum geometric factors listed above will rarely be achieved (except in the perigee case), because the source regions are usually smaller than the maximum individual-pinhole solid angles $s^2/f^2$. As was mentioned above, PIXIE can trade off angular response against sensitivity by varying the size of the pinholes. The angular resolution element is approximately $s/f$. There is nothing to be gained by reducing $s$ below 0.2 cm, because this is the approximate position resolution of the detector. For calculating counting rates it is necessary to take into account the detection efficiency of the proportional counter. Imaging a typical diffuse aurora (3 keV Maxwellian electron spectrum with an energy flux of 2 ergs cm$^{-2}$ sr$^{-1}$, corresponding to 1.3 kR at 427.8 nm) from a distance of 8 Earth Radii, with the high-altitude pinhole set having $s$ = 0.2 cm, results in a counting rate per angular resolution element in the final summed image of approximately 0.1 per second provided that the source fills the pinhole solid angle. The solid angle corresponds to a square about 500 km on a side at the source distance.

### 3.8. CALIBRATION

Our knowledge of the sensitivity, spatial resolution, and spectral response of the PIXIE instrument all depend upon a thorough calibration program. The instrument sensitivity depends on both the detector efficiency as a function of energy and the camera geometry. Accordingly, in addition to the efficiency, we must determine the pinhole configuration as a function of the commanded aperture-plate position. The spatial resolution, spectral response, and absolute detector efficiency are all determined in a calibration program that makes use of small radioactive sources of known strength and comparison of laboratory data with calculations. In addition, the spectral response and detector efficiency, both of which may vary from point to point in the detector, can be checked in flight through the use of weak on-board

X-ray emitting radioactive sources. The daughter species of $Fe^{55}$, $Mn^{55}$, emits a 5.9 keV X-ray that is detected in the front chamber, and $Ag^{109}$, the daughter species of $Cd^{109}$, emits a 22-keV X-ray that is detected in the rear chamber.

The spatial response of the PIXIE camera was determined by using $Fe^{55}$ and $Cd^{109}$ sources at a distance of 1 m in front of the camera aperture plates. These small sources projected images of the opened pinholes on the detector. The physical size of the sources made a contribution to the blurring of the images that was smaller than the fundamental detector pixel diameter (0.7 mm) and approximately a factor of three smaller than the expected spatial resolution of the detector (2 mm); thus they were effectively point sources. A precision $x-y$ translator was used to position the sources at various locations in a plane perpendicular to the camera axis so that the entire detector was illuminated in the course of the testing. Thus, we are able to determine the spatial resolution throughout the detector volume. Well over 100 multiple-pinhole images were taken in the course of this calibration program. The analysis of these data is expected to require several months of effort that is only beginning at the time of this writing. When the instrument has undergone its final prelaunch refurbishment, the spatial-resolution calibration will be repeated.

The detector energy calibration cannot be performed until after the instrument refurbishment is completed, after the detectors have been purged, cleaned, and filled with the gas loads that will be used in flight. Then we will use radioactive sources and X-ray filters to measure the gain and energy resolution of each detector at three or more different energies. The filters are chosen primarily to absorb weak $K_\beta$ X-ray lines that lie at slightly higher energies than the $K_\alpha$ lines that are primary calibration lines for electron-capture sources such as $Fe^{55}$ and $Cd^{109}$. Long data-acquistion periods (approximately 24 hours) will be used to allow us to accumulate enough X-ray events to allow the detector to be calibrated on a spatial scale of approximately 3 mm square ($x$ and $y$) and one layer (1.1 cm) thick.

Calibration of the aperture plate configuration is a much simpler problem than the detector calibration. The open area of each pinhole is measured for a number of different aperture-plate command addresses. Measurement of each pinhole for three different command addresses for which the pinhole is at least partially opened enables us to determine the open area for all addresses. The results of the calibration indicate that the fixed and moving plates are aligned to one another within an error of approximately 0.1 mm in the direction perpendicular to their direction of travel (this is the direction in which no adjustment can be made) and that the pinhole arrays of the two plates are parallel within approximately 1 milliradian. The hole sizes are repeatable within the accuracy of the measurements, again approximately 0.1 mm.

## 4. Operations

The PIXIE instrument is mounted on the despun platform in order to provide continuous viewing of the Earth. It can be operated in any of the following modes, selected for optimization of data collection in various parts of the POLAR spacecraft's 1.8 $R_E \times 9$ $R_E$ orbit:

Normal Mode: auroral X-ray imaging from high altitude.

Standby Mode: detector high voltage off when POLAR is in radiation belts.

Perigee Mode: auroral X-ray quick snapshots when POLAR is outside radiation belts and near perigee.

Calibration Mode: same as Normal Mode except pinholes are closed and calibration sources are exposed to the detector.

Aperture Select Mode: movable plate is repositioned to change field of view or spatial resolution. Detector mode is same as Normal Mode or same as Standby Mode if POLAR is in radiation belts, but data will be of no scientific value in this mode.

Dual Mode: same as Normal Mode except the two aperture plates have different spatial resolution.

In all of the PIXIE modes, except for Standby Mode (or Aperture Select Mode while the satellite is in the radiation belts), the PIXIE event data stream is the same: 24 bits of information for an X-ray event are read out in three consecutive satellite telemetry-stream bytes every 7.36 ms, for a total of 135.87 events per second, evenly spaced in time. In the two excepted modes, the PIXIE event-data telemetry stream is utilized by the SEPS instrument on the despun platform and PIXIE neither generates nor telemeters event data. The PIXE housekeeping data stream is unaffected by PIXE mode selection.

## 5. The PIXIE Key Parameter Data Set

A PIXIE Key Parameter Data (KPD) Set will be established and maintained at the NASA Central Data Handling Facility (CDHF). The purpose of the PIXIE KPD Set is to provide timely calibrated data from PIXIE to the science community in a form that is easily interpreted. As such, the PIXIE KPD consists of processed data that summarize the key parameters of auroral X-ray emissions, including information on spatial, spectral and temporal variability. It is anticipated that the KPD will be used by the science community to identify geophysical events that warrant further study using all of the information available in the PIXIE telemetry.

The PIXIE KPD will consist of three types of data files. Plot Files contain data elements formatted as line plots, Image Files contain periodic subsets of PIXIE X-ray images, and Digital Files contain all of the processed data products in digital format. Table II identifies the specific parameters contained in each of these files, along with their respective file structure and time resolution.

TABLE II

## Digital Files

| Parameter | Array Content | Time Resolution |
|---|---|---|
| X-ray Source Array (XSA) | 20x20 spatial pixels<br>8 energy channels | 10 minutes |
| X-ray Source Array 1 (XSA1) | 20x20 spatial pixels<br>Energy below 10 keV | 10 minutes |
| X-ray Source Array 2 (XSA2) | 20x20 spatial pixels<br>Energy above 10 keV | 10 minutes |
| Total X-ray Flux 1 (TXE1) | Total x-ray flux below 10 keV | 10 minutes |
| Total X-ray Flux 2 (TXE2) | Total x-ray flux above 10 keV | 10 minutes |

## Image Files

| Parameter | Array Content | Time Resolution |
|---|---|---|
| X-ray Source Array 1 (XSA1) | 20x20 image<br>Energy below 10 keV | 60 minutes |
| X-ray Source Array 2 (XSA2) | 20x20 image<br>Energy above 10 keV | 60 minutes |

## Plot Files

| Parameter | Array Content | Time Resolution |
|---|---|---|
| Total X-ray Flux 1 (TXE1) | Total x-ray flux below 10 keV | 10 minutes,24-hr period |
| Total X-ray Flux 2 (TXE2) | Total x-ray flux above 10 kev | 10 minutes, 24 hr period |

In order to produce the KPD, the PIXIE telemetry data are reduced in volume by accumulating over a selected time interval. The accumulation time interval selected for digital files is 10 min. The accumulated data are binned into three-dimensional arrays (called X-ray source arrays) that sort the detected X-rays according to energy and location. The arrays consist of 8 energy channels and $20 \times 20$ spatial arrays that identify the X-ray source location within the image plane. Orbital and attitude data can be used to assign each of the 400 image elements to a terrestrial source location. These source arrays are also used to generate X-ray image files for the KPD data base at one-hour intervals.

In addition to the X-ray source array, the KPD digital file contains two arrays that include X-ray fluxes integrated over two broad energy ranges. One of the images uses data from the front chamber integrating X-ray fluxes below 12 keV, and the second uses data from the rear chamber, integrating X-rays above 10 keV. These integrated flux values are provided as line plots covering 24-hour intervals with 10-min resolution. It is anticipated that combinations of the X-ray images and the integrated flux plots will provide the user with enough information on the spatial, temporal and spectral features of auroral events to identify events for further detailed analysis.

## 6. Summary

PIXIE is designed to image simultaneously the entire auroral region from high altitudes, measuring the spatial distribution and temporal variation of auroral X-ray emission in the 2 to 60 keV energy range. Bremsstrahlung spectra are independent of atmospheric chemistry and are unaffected by transmission through the upper atmosphere. While the other imagers offer higher spatial resolution, PIXIE provides spectra that are easily interpreted over all local times. The three imaging experiments aboard the POLAR satellite promise to provide unprecedented opportunities to study the electrodynamics of the polar atmosphere.

## Acknowledgements

We wish to thank our co-investigators D. L. Chenette, H. D. Voss, P. Mizera, M. Walt, and J. G. Luhmann for their contributions. We also thank J. B. Reagan, D. Cauffman and W. Calvert for their great help in the early phases of the program. We also appreciate greatly the efforts at Lockheed of P. S. Baker, M. B. Bumala, V. Chinn, B. J. Costanzo, T. R. Fisher, M. J. Froemke, E. E. Gaines, C. Gilbreth, R. W. Griswold, M. Hilsenrath, H. G. Lane, E. L. McFeaters Jr., G. S. Orsten, M. L. Peloquin, P. J. Pomeroy, L. A. Reed, R. Robinson, G. T. Saavedra, K. G. Strickler, J. D. Tracey. At Aerospace we appreciate the contributions of R. F. Gerardi, J. F. Kirshman, and M. McNab. We also appreciate the efforts of P. DeMent, J. Giganti

and E. Knouse at the University of Maryland. The Bergen group appreciates greatly the contribution of K. Slettebakken. The contribution of the University of Bergen was supported by The Research Council of Norway. The Lockheed and Maryland contributions to this effort were supported by NASA under contract NAS5-30372 and the Aerospace support was provided by NASA under contract NAS5-30369. We appreciate the assistance of W. Anselm, J. Hrastar, T. Taylor, D. Crosby and K. Sizemore at the NASA Goddard Space Flight Center, and P. A. Harris at the Martin Marietta Corporation.

## References

Ahn, B. H., Kroehl, H. W., Kamide, Y., and Gorney, D. J.: 1989, *J. Geophys. Res.* **94** 2565.
Calvert, W., Voss, H. D., and Sanders, T. C.: 1983, *IEEE Trans Nucl. Sci.* **NS-32**, 112.
Cannon, T. M. and Fenimore, E. E.: 1978, *IEEE Trans. Nucl. Sci.* **NS-25**, 184.
Chenette, D. L., Datlowe, D. W., Imhof, W. L., Schumaker, T. L., and Tobin, J. D.: 1992, *SPIE Proceedings* **16**, 1745,.
Datlowe, D. W., Imhof, W. L., and Voss H. D.: 1988, *J. Geophys. Res.* **93**, 8662.
Gilvin, P. G., Mathieson E., and Smith, G. C.: 1981, *Nucl. Instr. Methods* **185**, 595.
Gorney, D. J.: 1987, in Y. Kamide and R. Wolf (eds.), *Quantitative Modeling of Magnetospheric-Ionosphere Coupling Processes*, Kyoto Sangyo University, Kyoto, Japan, p. 197.
Imhof, W. L.: 1981, *Space Sci. Rev.* **29**, 201.
Imhof, W. L., Nakano, G. H., Johnson, R. G., and Reagan, J. B.: 1974, *J. Geophys. Res.* **79**, 565.
Imhof, W. L., Voss, H. D., Datlowe, D. W., and Mobilia, J.: 1985, *J. Geophys. Res.* **90**, 6515.
Mathieson, E., Smith, G. C., and Gilvin, P. G.: 1980, *Nucl. Instr. Methods* **174**, 221.
Mauk, B. H., Chin, J., and Parks, G.: 1981, *J. Geophys. Res.* **86**, 6827.
Mertz, L. and Young, N.: 1961, *Proceedings of the International Conference on Optical Instruments and Techniques*, Chapman and Hall, London, p. 305.
Miller, K. L. and Vondrak, R. R.: 1985, *Radio Science* **20**, 431.
Mizera, P. F., Luhmann, J. G, Kolansinski, W. A., and Blake, J. B.: 1978, *J. Geophys. Res.* **83**, 5573.
Mizera, P. F., Gorney, D. J., and Roeder, J. L.: 1984, *Geophys. Res. Letters* **11**, 255.
Skinner, G. K., Eyles, C. J., Willmore, A. P., Bertram, D., Church, M. J., Herring, J. R. H., Ponman, T. J., and Watt, M. P.: 1988, *Astrophys. Letters Commun.* **27**, 199.
Yamagami, T. *et al.*: 1990, *J. Geomag. Geoelectr.* **42**, 1175.